Delta-Connected Static Var Compensator (SVC) based Hybrid Active Power Filter (SVC-HAPF) and Its Control Method

Lei Wang[1], Keng-Weng Lao[1], Chi-Seng Lam[2] and Man-Chung Wong[1,2]
1 - Department of Electrical and Computer Engineering, Faculty of Science and Technology, University of Macau, Macau, China
2 - State Key Laboratory of Analog and Mixed-Signal VLSI, University of Macau, Macau, China
E-mail: cslam@umac.mo / C.S.Lam@ieee.org

***Abstract*-In this paper, a new structure and the coordinated control method of a delta connected static var compensator (SVC) based hybrid active power filter (SVC-HAPF) for reactive current, harmonic current and unbalanced current compensation are proposed. The proposed delta-connected SVC-HAPF has the desirable characteristics of wide compensation range with low voltage/current rating requirement in the active inverter part. Simulation results are provided to verify the effectiveness of the proposed structure and control method.**

***Index Terms*—Current harmonics, static var compensator (SVC), hybrid active power filter (HAPF), reactive power, static var compensator based hybrid active power filter (SVC-HAPF)**

I. Introduction

MAJORpower quality issues of the medium-voltage distribution systems are low power factor, harmonic pollution and unbalanced problem. In order to solve the above power quality issues, power quality compensators such as static var compensator (SVCs) and active power filters (APFs) have been widely applied in the medium-voltage applications. The SVCs can improve power factor and compensate unbalanced current [1]-[4]. However, SVCs inject harmonic current to system during operation and do not have any harmonic current compensation ability [5]. On the other hand, the star-connected APFs can compensate the above three current quality issues and have been proposed. However, both voltage and current ratings of the active inverter part of the APFs are high, which drive up their initial and operation cost. In order to reduce the voltage rating of the active inverter part, the star-connected static var compensator based hybrid active power filters (SVC-HAPFs) have been proposed in [6]-[12]. However, the star-connected SVC-HAPFs still suffer from the high current rating requirement of the active inverter part. In this paper, the structure and control method of a delta-connected SVC-HAPF has been proposed as in Fig. 1.The idea of the delta-connected compensator aims to reduce the compensation current in each phase under unbalanced load. For example, a STATCOM with delta-connected inverter is being proposed to compensate the negative sequence current caused by the unbalanced load [13]-[15]. In 2012, a STATCOM based on modular multilevel cascade converter is proposed to accomplish negative-sequence reactive-power control [14]. In 2015, a harmonic reference current balancing method is proposed for delta-connected static synchronous compensator [15]. However, the compensation capability is not flexible enough in these studies. Compared with the traditional star-connected APFs and SVC-HAPFs, the proposed delta-connected SVC-HAPF provides extra flexibility in unbalanced current compensation by controlling the circulating currents flowing inside the structure, and the current rating can be reduced to $1/\sqrt{3}$.

In this paper, the system configuration of the proposed delta connected SVC-HAPF is introduced in Section II. In Section III, the control strategy of the delta connected SVC-HAPF is presented. Finally, simulation results (Section IV) are provided to prove the advantages of the proposed delta-connected SVC-HAPF.

II. Circuit Configuration of the Proposed Delta-Connected SVC-HAPF

Fig. 1 shows the circuit configuration of the delta-connected SVC-HAPF, in which the subscript "*x*" stands for phase *a*, *b,* and *c* in the following analysis. v_{sx} and v_x are the source and load voltages; i_{sx}, i_{Lx}, and i_{cx} are the source, load, and compensating currents, respectively. L_s is the transmission line impedance. The delta-connected SVC-HAPF consists of a SVC part and an active inverter part.

The SVC part is composed of a coupling inductor L_c, a parallel capacitor C_{PF}, and a thyristor-controlled reactor with L_{PF}. The SVC part provides a wide and continuous inductive and capacitive reactive power compensation range that is controlled by controlling the firing angles α_x of the thyristors. The active inverter part is composed of a voltage source inverter with a DC-link capacitor C_{DC}, and the small rating active inverter part is used to improve the compensation

This work was financially supported in part by the Science and Technology Development Fund, Macao SAR (FDCT) (109/2013/A3, 025/2017/A1) and in part by the Research Committee of the University of Macau (MYRG2015-00009-FST, MRG012/WMC/2015/FST, MYRG2015-00030-AMSV, MYGR2017-00038-FST)

978-1-5386-1127-2/17/$31.00 ©2017 IEEE

performance of the SVC part and compensate the harmonics currents.

Based on the circuit system configuration in Fig. 1, the control strategy of the delta connected SVC-HAPF will be discussed in next section.

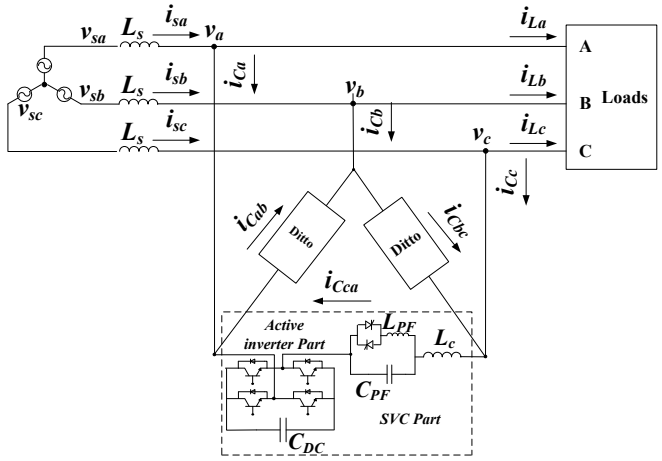

Fig. 1. The proposed delta-connected SVC-HAPF

III. Control Strategy for Delta-connected SVC-HAPFs

In this section, a control strategy for the delta-connected SVC-HAPFs is proposed by coordinating the control of the TCLC part and the active inverter part, so that the two parts can complement each other's disadvantages and the overall performance of the delta-connected SVC-HAPF can be improved. In the following, the control strategy of the delta-connected SVC-HAPFs is discussed. The discussion is separated into two parts: *A.* TCLC control and *B*. active inverter control. And the overall control block diagram of the SVC-HAPF is shown in Fig. 2.

A. TCLC part control

The purpose of the TCLC part is used to compensate the fundamental reactive power and unbalanced power by providing different firing angles for each SVC part. In order to obtain firing angles of SVC part, the SVC part impedance X_{xy} (x and y stand for phase *a, b* or, *c*) in real time is calculated first. The expression of X_{xy} can be rewritten as:

$$\begin{bmatrix} X_{ab} \\ X_{bc} \\ X_{ca} \end{bmatrix} = \begin{bmatrix} \frac{3 \cdot V_x^2}{Q_{ab}^c} \\ \frac{3 \cdot V_x^2}{Q_{bc}^c} \\ \frac{3 \cdot V_x^2}{Q_{ca}^c} \end{bmatrix} = \begin{bmatrix} \frac{3 \cdot V_x^2}{Q_{Lc} - Q_{La} - Q_{Lb}} \\ \frac{3 \cdot V_x^2}{Q_{La} - Q_{Lb} - Q_{Lc}} \\ \frac{3 \cdot V_x^2}{Q_{Lb} - Q_{Lc} - Q_{La}} \end{bmatrix} \quad (1)$$

where V_x is the rms value of the load voltage, Q_{Lx} is the phase load reactive power (x stands for phase *a*, *b* or, *c*). The V_x and $Q_{Lx} \approx -\bar{q}_{Lx}/2$ can be calculated in real-time as:

$$\begin{bmatrix} q_{La} \\ q_{Lb} \\ q_{Lc} \end{bmatrix} = \begin{bmatrix} v_a \cdot i_{La}^D - v_a^D \cdot i_{La} \\ v_b \cdot i_{Lb}^D - v_b^D \cdot i_{Lb} \\ v_c \cdot i_{Lc}^D - v_c^D \cdot i_{Lc} \end{bmatrix} \quad (2)$$

$$V_x = \|v\| / \sqrt{3} = \sqrt{v_a^2 + v_b^2 + v_c^2} / \sqrt{3} \quad (3)$$

where v_x^D and i_{Lx}^D can be obtained by delaying v_x and i_{Lx} by a phase angle of 90^o. q_{Lx} is the phase instantaneous reactive power. Then $Q_{Lx} \approx -\bar{q}_{Lx}/2$ can be obtained by passing the q_{Lx} in (2) though low pass filters (LPFs). $\|v\|$ is the norm of the three-phase instantaneous load voltage. After obtaining the SVC impedance X_{xy} through (1)-(3), the firing angle α_{xy} can be determined by solving the equation below.

$$\begin{bmatrix} X_{ab}(\alpha_{ab}) \\ X_{bc}(\alpha_{bc}) \\ X_{ca}(\alpha_{ca}) \end{bmatrix} = \begin{bmatrix} \frac{\pi X_{L_{PF}} X_{C_{PF}}}{X_{C_{PF}}[2\pi - 2\alpha_{ab} + \sin(2\alpha_{ab})] - \pi X_{L_{PF}}} + X_{L_c} \\ \frac{\pi X_{L_{PF}} X_{C_{PF}}}{X_{C_{PF}}[2\pi - 2\alpha_{bc} + \sin(2\alpha_{bc})] - \pi X_{L_{PF}}} + X_{L_c} \\ \frac{\pi X_{L_{PF}} X_{C_{PF}}}{X_{C_{PF}}[2\pi - 2\alpha_{ca} + \sin(2\alpha_{ca})] - \pi X_{L_{PF}}} + X_{L_c} \end{bmatrix} \quad (4)$$

where α_{xy} is the firing angle for SVC part, X_{L_c} , $X_{C_{PF}}$ and $X_{L_{PF}}$ are the impedances of the coupling inductor, the SVC capacitor and inductor (as Fig. 1), respectively. With the calculated X_{xy} from (1)-(3), the firing angle α_{xy} can be determined by solving (4). Since (4) has a term of $-2\alpha_{xy}+sin(2\alpha_{xy})$ and it does not have a closed-form solution. Therefore, a look-up table (LUT) is installed inside the controller. The trigger signals can be generated by comparing the firing angle α_{xy} with the phase angle of the load voltage θ_x to control the SVC part. And, θ_x can be obtained by using a phase lock loop (PLL).

B. Active inverter part control

The active inverter part is used to improve the TCLC part characteristic and compensate the current harmonics by limiting the compensating current i_{Cx} to its reference value i_{Cx}^*.For the delta-connected structure, the reference phase compensating current i_{Cx}^* is required to transfer to the line-to-line reference current i_{Cxy}^* in order to get the trigger signals for active inverter part. And the transform function can be expressed as [16]:

$$\begin{bmatrix} i_{Cab}^* \\ i_{Cbc}^* \\ i_{Cca}^* \end{bmatrix} = \frac{1}{3} \cdot \begin{bmatrix} 1 & -1 & 0 \\ 1 & 2 & 0 \\ -2 & -1 & 0 \end{bmatrix} \cdot \begin{bmatrix} i_{Ca}^* \\ i_{Cb}^* \\ i_{Cc}^* \end{bmatrix} \quad (5)$$

In (5), the reference phase compensating current i_{Cx}^* can be obtained by using the instantaneous active and reactive current i_d-i_q method. And the reference i_{Cx}^*can be calculated as:

$$\begin{bmatrix} i_{Ca}^* \\ i_{Cb}^* \\ i_{Cc}^* \end{bmatrix} = \sqrt{\frac{2}{3}} \cdot \begin{bmatrix} 1 & 0 \\ -1/2 & \sqrt{3}/2 \\ -1/2 & -\sqrt{3}/2 \end{bmatrix} \cdot \begin{bmatrix} \cos\theta_a & -\sin\theta_a \\ \sin\theta_a & \cos\theta_a \end{bmatrix} \cdot \begin{bmatrix} \tilde{i}_d \\ i_q \end{bmatrix} \quad (6)$$

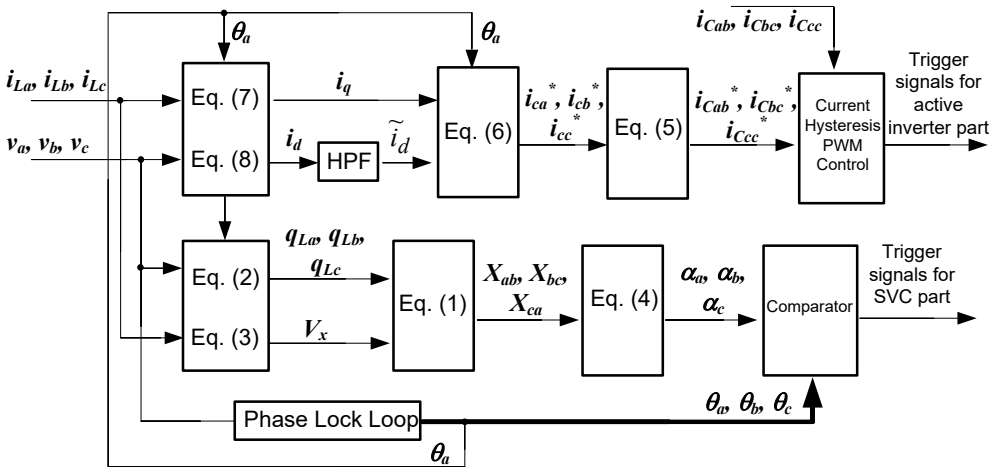

Fig. 2. The overall control block of the delta-connected SVC-HAPF

where i_d and i_q are the instantaneous active and reactive current, which contain both DC components and AC components. The AC component $\tilde{i}_d$ is obtained by passing i_d through a high-pass filter (HPF). And i_d and i_q can be obtained as:

$$\begin{bmatrix} i_d \\ i_q \end{bmatrix} = \begin{bmatrix} \cos\theta_a & \sin\theta_a \\ -\sin\theta_a & \cos\theta_a \end{bmatrix} \cdot \begin{bmatrix} i_\alpha \\ i_\beta \end{bmatrix} \tag{7}$$

In (7), the i_α and i_β in α–β plane are transformed from the load current in *a*-*b*-*c* plane as:

$$\begin{bmatrix} i_\alpha \\ i_\beta \end{bmatrix} = \begin{bmatrix} 1 & -1/2 & -1/2 \\ 0 & \sqrt{3}/2 & -\sqrt{3}/2 \end{bmatrix} \cdot \begin{bmatrix} i_{La} \\ i_{Lb} \\ i_{Lc} \end{bmatrix} \tag{8}$$

Referring to the equations (5)-(8) above, the reference current i_{Cxy}^* can then be obtained. By comparing the i_{Cxy}^* with the i_{Cxy} (measured by transducers), the trigger signal for the active inverter part can be generated by using the current hysteresis PWM method.

Based on the discussion above, the overall control block diagram of the delta-connected SVC-HAPF is shown in Fig. 2.

IV. Simulation Results

The system configuration for the proposed delta-connected SVC-HAPF simulation is shown in Fig. 1 and the SVC-HAPF with low dc-link voltage (V_{DC}=90V) is connected to a 380 V grid. The simulation results are obtained using PSCAD/EMTDC.

Fig. 3 shows the simulated waveforms of the load voltages, dc-link voltage, load and source currents for balanced harmonic inductive and capacitive loads by using the delta-connected SVC-HAPF compensation. At 40ms, the capacitive load is connected to the system. And, Fig. 4 shows the corresponding harmonic spectrums of the load and source currents. Fig. 5-Fig. 7 show the simulated waveforms, source current harmonic spectrums and phasor diagrams of the source voltages and currents under unbalanced loads compensation by using the delta-connected SVC-HAPF. And the simulation results are summarized in Table I. At 40ms, capacitive loads are connected and causes disturbance on the load current.

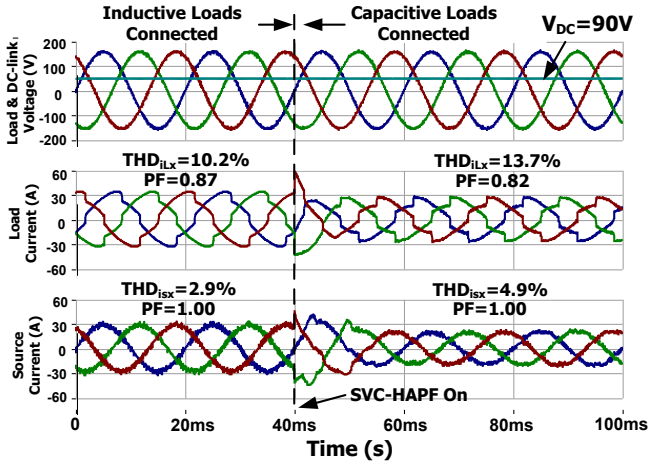

Fig. 3. Simulated waveforms of the load voltages, dc-link voltage, load current and source current for inductive and capacitive loads by using the delta-connected SVC-HAPF compensation under balanced harmonic loads

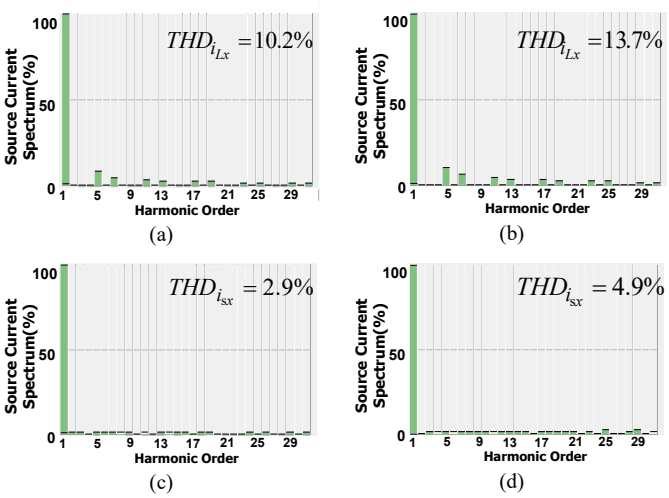

Fig. 4. Current harmonic spectrums of source current for: (a) inductive loads before compensation, (b) capacitive loads before compensation, (c) inductive loads after compensation and (d) capacitive loads current after compensation

The purpose of

Fig. 3 is to verify the dynamic performance of SVC-HAPF due to the loads changing situation. And, the loads are changing from capacitive to inductive at 40ms.From

Fig. 3 and Table I, after the delta-connected SVC-HAPF compensation, the source power factors (PFs) are compensated to unity from the original 0.87 and 0.82 for inductive and capacitive loads by using the delta connected SVC-HAPF compensation. From

Fig. 3, Fig. 4 and Table I, it can be seen that the source current THD_{isx} are improved from 10.2% and 13.7% to 2.9% and 4.9%. Based on Table I, it can be seen that the current passing through the delta-connected SVC-HAPF (I_{Cxy}) can be reduce to $1/\sqrt{3}$ time of the compensating current (I_{Cx}). And the dc-link voltage can keep at the low level (V_{DC}=90V for 380V system) for both inductive loads and capacitive loads compensations.

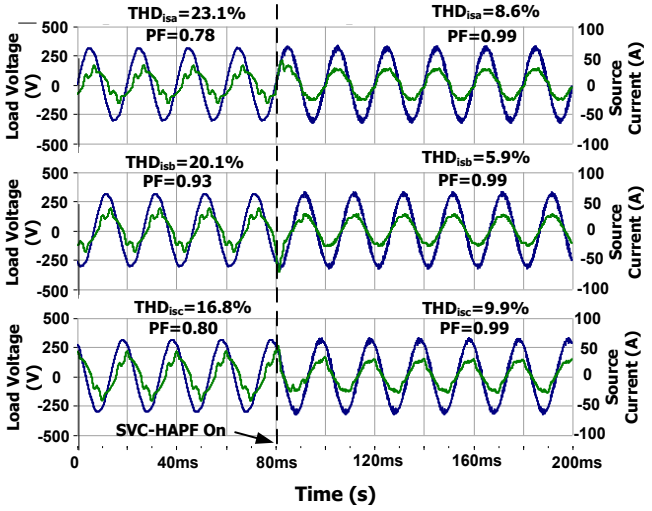

Fig. 5. Simulated waveforms of the load voltages and currents with the delta-connected SVC-HAPF compensation under unbalanced harmonic loads

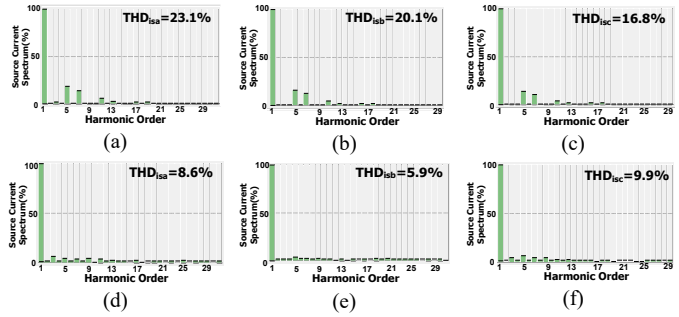

Fig. 6. Current harmonic spectrums of source currents: before compensation (a) phase *a*, (b) phase *b*, (c) phase *c*; after the SVC-HAPF compensation (d) phase *a*, (e) phase *b*, (f) phase *c*

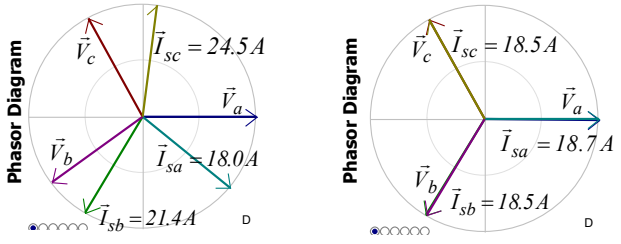

(a) (b)

Fig. 7. Phasor diagrams of source voltages and currents: (a) before compensation and (b) after the SVC-HAPF compensation under unbalanced harmonic loads

From Fig. 5, it can be seen that after the delta-connected SVC-HAPF compensation, the source PFs are compensated to 0.99 from the original 0.78, 0.93 and 0.80. From Fig. 5 and Fig. 6, it can be seen that the source current THD_{isx} are improved from 23.1% to 9.9% for the worst phase. Based on Fig. 5 and Fig. 7, it can be seen that the source current i_{sx} and the load voltage v_x are compensated to be in phase with each other under unbalanced loads case. Based on Table I, it can be seen that the current passing through the delta-connected SVC-HAPF (I_{Cxy}) is smaller than the compensating current (I_{Cx}). And the dc-link voltage can keep at the low level (V_{DC}=90V) for unbalanced loads compensation.

Table I
Simulation results for different loads compensation before and after delta connected SVC-HAPF compensation

			Q_{sx} (var)	PF	I_{sx} (A)	I_{Cx}/I_{Cxy} (A)	THD_{isx} (%)	V_{DC} (V)
Balanced Loads	Before Comp.		2458	0.87	22.7	--	10.2	--
	SVC-HAPF		2	1.00	19.9	11.6/6.7	2.9	90
	Before Comp.		-2145	0.82	17.5	--	13.7	--
	SVC-HAPF		1	1.00	14.6	10.2/5.8	4.9	90
Unbalanced Loads	Before Comp.	A	2443	0.78	18.2	--	23.1	--
		B	1727	0.93	21.3	--	20.1	
		C	3163	0.80	24.2	--	16.8	
	SVC-HAPF	A	3	0.99	18.6	12.7/4.9	8.6	90
		B	5	0.99	18.6	8.6/6.1	5.9	
		C	4	0.99	18.6	14.8/10.4	9.9	

**Notes the shades areas mean undesirable results*

V. Conclusions

This paper proposes a new structure and control method of the delta-connected SVC-HAPF for reactive current, harmonic current and unbalanced current compensation. The proposed delta-connected SVC-HAPF has the desirable characteristics of wide compensation range (from inductive to capacitive) with low dc-link operating voltage. Simulation results validate the proposed delta-connected SVC-HAPF can effectively compensate reactive current, harmonic current and unbalanced current with low current passing through delta-connected SVC-HAPF and low dc-link voltage (V_{DC}=90V for 380V system).

References

[1] M. M Li, W. L Li, J. Zhao, W. Chen, W. T Yao, "Three-layer coordinated control of the hybrid operation of static var compensator and static synchronous compensator," *IET Generation, Transmission & Distribution*, vol. 10, no. 9, pp. 2185-2193, Sept. 2016.

[2] Sam Morello, Thomas J. Dionise, Thomas L. Mank, "Comprehensive Analysis to Specify a Static Var Compensator for an Electric Arc Furnace Upgrade," *IEEE Trans. Ind. Appl.*, vol. 51, no. 6, pp. 4840-4852, Dec., 2015.

[3] L. B. Garcia Campanhol, S. A. Oliveira da Silva and A. Goedtel, "Application of shunt active power filter for harmonic reduction and reactive power compensation in three-phase four-wire systems," *IET Power Electron.*, vol. 7, no. 11, pp. 2825-2836, Nov., 2014.

[4] R. Panigrahi, B. Subudhi and P. C. Panda, "A Robust LQG Servo Control Strategy of Shunt-Active Power Filter for Power Quality Enhancement," *IEEE Trans. Power Electron.*, vol. 31, no. 4, pp. 2860-2869, April 2016.

[5] L. Wang, C. S. Lam, and M. C. Wong, "Design of a thyristor controlled LC

compensator for dynamic reactive power compensation in smart grid," *IEEE Trans. Smart. Grid*.vol. 8, no. 1, pp. 409-417, Jan. 2017.

[6] L. Wang, C. S. Lam, and M. C. Wong "An unbalanced control strategy for a thyristor controlled LC-coupling hybrid active power filter (SVC-HAPF) in three-phase three-wire systems," *IEEE Trans. Power Electron.*, vol. 32, no. 2, pp. 1056-1069, Feb. 2017.

[7] S. Rahmani, A. Hamadi, and K. Al-Haddad, "A combination of shunt hybrid power filter and thyristor-controlled reactor for power quality," *IEEE Trans. Ind. Electron.,* vol. 61, no. 5, pp. 2152 - 2164, May 2014.

[8] L. Wang, C. S. Lam, and M. C. Wong, "A hybrid-STATCOM with wide compensation range and low dc-link voltage," *IEEE Trans. Ind. Electron.,* vol. 63, no. 6, pp. 3333-3343, Jun. 2016.

[9] L. Wang, C. S. Lam, and M. C. Wong, "Hardware and software design of a low dc-link voltage and wide compensation range thyristor controlled LC-coupling hybrid active power filter," *TENCON 2015 IEEE Region 10 Conference proceeding*s, Nov. 2015.

[10] L. Wang, C. S. Lam, M. C. Wong, "Modeling and parameter design of thyristor controlled LC-coupled hybrid active power filter (SVC-HAPF) for unbalanced compensation," *IEEE Trans. Ind. Electron.*, vol. 64, no. 3, pp. 1827-1840, Mar. 2017.

[11] L. Wang, C. S. Lam and M. C. Wong, "Selective Compensation of Distortion, Unbalanced and Reactive Power of a Thyristor-Controlled LC -Coupling Hybrid Active Power Filter (TCLC-HAPF)," *IEEE Trans. Power Electron.*, vol. 32, no. 12, pp. 9065-9077, Dec. 2017.

[12] C. S. Lam, L. Wang, S. I. Ho, M. C. Wong, "Adaptive thyristor controlled LC – hybrid active power filter for reactive power and current harmonics compensation with switching loss reduction," *IEEE Trans. Power Electron.*, vol. 32, no. 10, pp. 7577-7590, Oct. 2017

[13] Y. Yu, G. Konstantinou, C. D. Townsend, R. P. Aguilera, V. G. Agelidis, "Delta-connected cascaded H-bridge multilevel converters for large-scale pv grid integration," *IEEE Trans. Ind. Electron.,* early access: doi: 10.1109/TIE.2016.2645885

[14] P. H. Wu, H. C. Chen, Y. T. Chang and P. T. Cheng, "Delta-connected cascaded H-bridge converter application in unbalanced load compensation," *IEEE Trans. Ind. Appl.,* vol. 53, no. 2, pp. 1254-1262, Mar-Apr. 2017.

[15] B. Wang, J. Shang, N. Dai and H. Chen, "Harmonic reference currents balancing method for delta-connected static synchronous compensator," *Electron. Letters,* vol. 51, no. 25, pp. 2134-2136, Oct. 2015

[16] V. Soares, P. Verdelho and G. D. Marques, "An instantaneous active and reactive current component method for active filters,"*IEEE Trans. Power Electron.*, vol. 15, no. 4, pp. 660-669, Jul 2000.